

## Conductance step for a single-atom contact in the scanning tunneling microscope: Noble and transition metals

C. Sirvent, J. G. Rodrigo, S. Vieira, L. Jurczyszyn,\* N. Mingo, and F. Flores

*Instituto de Ciencia de Materiales "Nicolás Cabrera," Universidad Autónoma de Madrid, E-28049 Madrid, Spain*

(Received 31 July 1995; revised manuscript received 27 February 1996)

Conductance steps for atomic point contacts of Au, Ni, and Pt have been measured. Jump-to-contact and jump-to-tunnel processes have been identified and their conductances measured. Differences between conductance steps for noble and transition metals are interpreted as being due to the  $d$  orbitals that, in transition metals, provide new channels to the electron conductance. This interpretation is supported by a theoretical analysis, which shows good agreement with the experimental data. [S0163-1829(96)03323-1]

### I. INTRODUCTION

Conductance experiments in atomic dimension contacts between metallic electrodes have been made recently using two different techniques: mechanically controllable break junctions<sup>1,2</sup> and scanning tunneling microscopy (STM).<sup>3-6</sup> Reports on different metals, at both liquid helium<sup>1-3</sup> and room temperature,<sup>4-6</sup> have been published. From those experiments, people have been able to measure the change in conductance due to the jump to contact (JC) during the controlled approach of the electrodes. Also the inverse process, i.e., the jump to tunnel (JT) when the tip and sample lose their physical contact, can be observed in the conductance measurements.

There exists evidence from experiments<sup>1,3</sup> and molecular dynamics calculations,<sup>7</sup> showing that in this process the minimum cross section of the contact can be that corresponding to a single atom. Some reports have claimed<sup>2,4,5</sup> that the observed first conductance steps, including that of the JC, are due to a purely geometrical change of cross section when the neck connecting the electrodes is elongated or contracted.<sup>8</sup> That is analogous to the well-known conductance quantization effect appearing in the gate formed at a microcontact in a two-dimensional gas.<sup>9</sup> Other theoretical and experimental reports<sup>1</sup> suggest, however, an interpretation that takes into account the electronic nature of the atom forming the neck. In this paper we address these questions, for which we have made a study of the JC and JT processes, for several metals, Au, Pt, and Ni, both experimentally and theoretically. Experimentally, we have identified and measured the first conductance step for these metals, while theoretically we have concentrated our discussion on elucidating the role played in this conductance step by the  $d$  orbitals; this problem is also relevant for understanding how these orbitals affect the tunneling current.<sup>10</sup>

### II. EXPERIMENTAL DATA

Measurements have been performed using a STM at 4.2 K, both in He gas atmosphere and in high vacuum. Tips and samples used in these experiments were obtained from high-quality polycrystalline materials.<sup>11</sup>

The curves of conductance versus tip-to-sample distance were made by measuring the current  $I$  as a function of the

$z$ -piezo displacement. Bias voltage is kept fixed at values ranging typically from 10 to 100-mV, and the STM feedback is switched off. For our setup the total cable-shunt resistance is about 2  $\Omega$ .

We studied areas of the sample for which clear and reproducible topographical images were obtained. Once the experimental area was selected, we collected for our analysis only curves for which high apparent barrier heights ( $\sim 3$  eV) were found. These barrier heights are characteristic of clean spots.<sup>12</sup>

The initial tip-to-sample distance corresponds to the standard topographical mode, with tunneling resistances in the range 10–100 M $\Omega$ . Then the feedback loop is switched off, the  $z$  piezo is moved cyclically with an amplitude between 5 and 10  $\text{\AA}$ , and the current versus displacement curves are measured. Both the amplitude and the  $z$ -piezo offset can be changed; a typical curve covers 4–5  $\text{\AA}$  in the tunneling regime and 4–6  $\text{\AA}$  in contact, showing a few conductance steps. These curves are visualized also at real time in an oscilloscope.

As commented above, our discussion will be centered on the process of formation and break of the contact. At room temperature, and due to the high atomic mobility, once the contact is broken, both electrodes suffer restructurings in their apexes, making it difficult to enter in register in the following JC approach. At liquid-helium temperature it is possible, however, to go backward and forward in successive formation and break the contact,<sup>13</sup> always keeping the interface in similar conditions. This is shown dramatically in Fig. 1, where the conductance of the point contact is measured as a function of the tip displacement in the JC and the JT regimes for Au. Other experimental facts, such as the thermal and piezoelectric creep reduction, make low-temperature conditions the appropriate ones for the experiments carried out in this work. Accordingly, the results presented in this paper have been collected at 4.2 K.

Figure 1 shows typical data for JC and JT processes. From these figures we have obtained the statistics of the first conductance step shown in Fig. 2. These curves have been deduced from several hundreds of measurements similar to the ones shown in Fig. 1. The statistics of these curves are calculated from the values of the conductance along the plateau of the first conductance step, with an appropriate factor

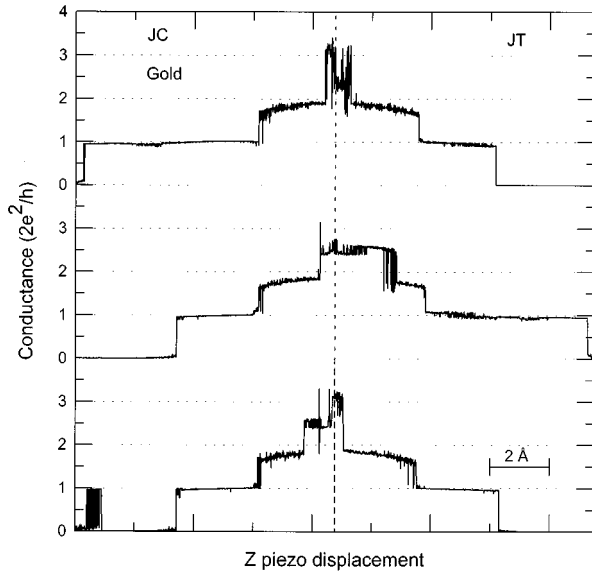


FIG. 1. Three conductances vs  $z$ -piezo displacement curves obtained on the same surface spot at 4.2 K for Au.

that gives identical weight to each individual measurement.

As can be observed from Fig. 2 the behavior of Au, Ni, and Pt is qualitatively different. Nickel shows for JC and JT a distribution of values with several peaks between one and

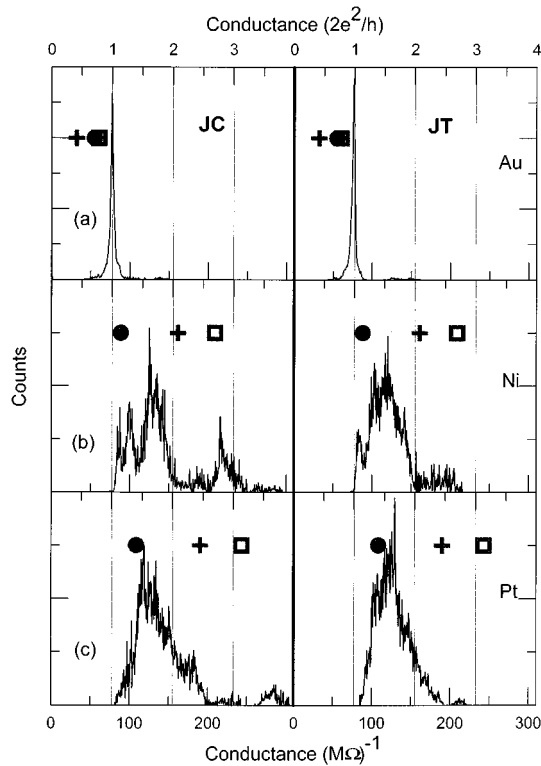


FIG. 2. Conductance values obtained from the first step just after the JT and before the JC (see Fig. 1). We have separated the JT (right side of the figure) from the JC (left side of the figure) in the statistics. The data are for Au (a), Ni (b), and Pt (c). We have also presented our theoretical results:  $\square$ , atomic configuration of Fig. 3(a),  $+$ , 3(b); and  $\circ$ , 3(c), for  $d=d_0$  ( $d_0$  is the metal nearest-neighbor distance).

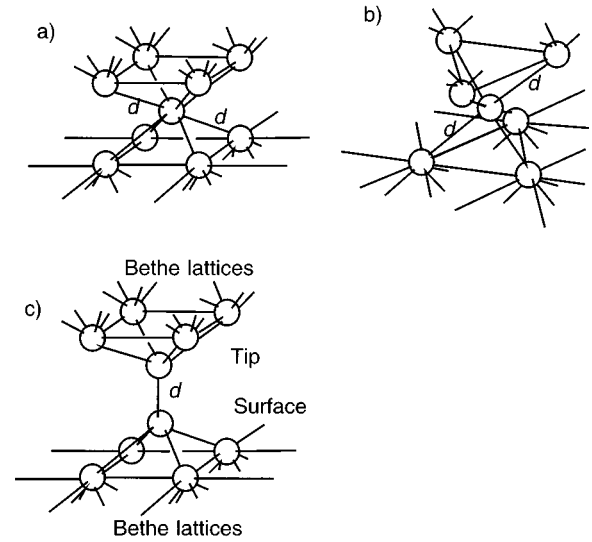


FIG. 3. Different geometries used to simulate the tip-sample interface in the JT and JC processes; (a) fourfold symmetry; (b) threefold symmetry; (c) contact of two equivalent atoms links the tip and the sample. Bethe lattices are used to simulate the tip and the sample density of states.

two quanta of conductance  $G_0$  ( $G_0=2e^2/h$ ). For JC there is a peak near  $3G_0$ , which is not observed in JT. Pt shows a behavior similar to that observed for Ni, although the conductance distribution for JC and JT peaks between  $G_0$  and  $2G_0$  and extends continuously to values larger than  $2G_0$ . Also a separated peak for JC appears near  $4G_0$ . In contrast to the transition metals reported here, Au presents a similar behavior for JC and JT, showing a peak close to (but slightly below)  $G_0$ .

### III. THEORETICAL MODEL

Our theoretical analysis will concentrate on the case of single-atom contact between the tip and the sample. Our main interest is to understand the effect that the  $d$  orbitals may have in the junction conductance. In this regard, instead of attempting a full molecular mechanics calculation, we have considered different *a priori* geometries that try to simulate the interface created along the JC and JT processes. As previous theoretical results<sup>14</sup> have shown, the conductance of a small contact depends mainly on the electronic and geometrical properties of the small neck formed around the center of the contact; accordingly we have modeled the atomic contact by introducing the geometries of Fig. 3, where a single atom is at the center of a small cluster having a threefold or a fourfold geometry [Figs. 3(a) and 3(b)]; also a contact of two atoms is introduced as shown in Fig. 3(c). In all these cases, the small clusters are joined to Bethe lattices<sup>15</sup> that model the electronic structure of the tip and the sample. The hypothesis that different geometries can take place for the same system is supported by the dispersion of experimental values of the conductance corresponding to the JC and the JT contacts in different materials (Fig. 2). Our study aims to give an explanation of these experimental data based on the possible different geometries of the tip apex.

The point contact conductance is calculated using a tight-

binding model<sup>16</sup> described by the following Hamiltonian:

$$\hat{H} = \hat{H}_T + \hat{H}_S + \hat{H}_{\text{int}}, \quad (1)$$

where  $\hat{H}_T$  and  $\hat{H}_S$  are the tip and sample Hamiltonians, respectively,

$$\hat{H}_T = \sum_{i,\sigma} E_i n_{i,\sigma} + \sum_{j,i,\sigma} T_{i,j} (c_{i,\sigma}^\dagger c_{j,\sigma} + c_{j,\sigma}^\dagger c_{i,\sigma}), \quad (2)$$

$$\hat{H}_S = \sum_{\alpha,\sigma} E_\alpha \hat{n}_{\alpha,\sigma} + \sum_{\alpha,\beta,\sigma} T_{\alpha,\beta} (c_{\alpha,\sigma}^\dagger c_{\beta,\sigma} + c_{\beta,\sigma}^\dagger c_{\alpha,\sigma}) \quad (3)$$

and  $\hat{H}_{\text{int}}$  defines the tip-sample coupling:

$$\hat{H}_{\text{int}} = \sum_{\alpha,i,\sigma} T_{\alpha,i} (c_{i,\sigma}^\dagger c_{\alpha,\sigma} + c_{\alpha,\sigma}^\dagger c_{i,\sigma}). \quad (4)$$

As discussed in previous papers,<sup>17</sup> Keldysh method<sup>18,19</sup> allows us to calculate nonequilibrium Green functions and, in particular, the tunneling current  $I$  between the tip and the sample. This theoretical analysis yields the following result:<sup>16</sup>

$$I = \frac{4\pi e}{\hbar} \int_{-\infty}^{\infty} d\omega \sum_{\alpha,\beta,\gamma,i,j,k} [T_{i,\alpha} \rho_{\alpha,\beta}^{(0)}(\omega) D_{\beta,\gamma}^R(\omega) \times T_{\gamma,j} \rho_{j,k}^{(0)}(\omega) D_{k,i}^A(\omega)] [f_T(\omega) - f_S(\omega)], \quad (5)$$

where  $f$  is the Fermi distribution function for each side of the interface, and

$$D_{k,i}^A = \left[ \delta_{k,i} - \sum_{j,l,m} T_{k,j} G_{j,l}^{A(0)} T_{l,m}^\dagger G_{m,i}^{A(0)} \right]^{-1}, \quad (6)$$

$$D_{\beta,\gamma}^R = \left[ \delta_{\beta,\gamma} - \sum_{\alpha,\omega,\delta} T_{\beta,\alpha} G_{\alpha,\omega}^{R(0)} T_{\omega,\delta}^\dagger G_{\delta,\gamma}^{R(0)} \right]^{-1} \quad (7)$$

in these equations  $G^{A(0)}$  and  $G^{R(0)}$  refer to the advanced and retarded Green functions of the uncoupled system (with  $T_{\alpha,i} = 0$ ). Equation (5) defines the total tunneling current as a function of  $T_{i,\alpha}$  and the electronic properties of the uncoupled tip and sample. For a small bias we can write

$$G = \frac{I}{V} = \frac{4\pi e^2}{\hbar} \sum_{\alpha,\beta,\gamma,i,j,k} T_{i,\alpha} \rho_{\alpha,\beta}^{(0)} D_{\beta,\gamma}^R T_{\gamma,j} \rho_{j,k}^{(0)} D_{k,i}^A. \quad (8)$$

This is the basic equation we are going to use to calculate the conductance of different tip-sample geometries. In our theoretical approach we have several orbitals per site. Typically we take  $s$ ,  $p$ , and  $d$  orbitals associated with the  $s$ ,  $p$ , and  $d$  bands of the metal we are considering. This means that the Green functions  $G^{A(0)}$  and  $G^{R(0)}$  have  $(9n \times 9n)$  components, where  $n$  is the number of atomic sites considered for each tip or sample cluster: notice that in our specific calculations, the Bethe lattices are projected onto the atoms forming the clusters shown in Fig. 3. We have assumed that for the investigated geometries all the tight-binding parameters coincide with the ones proposed for the metal bulk<sup>20</sup> if  $d$ , see Fig. 3, is taken equal to the nearest-neighbor distance of the crystal,  $d_0$ . Notice that for this particular case, the environment of each atom is very similar to the one found in the

bulk; then, we can expect the atom-atom distance near the interface to be very close to  $d_0$ . As a further step, we have changed  $d$  by  $\pm 10\%$  and modified accordingly the hopping interactions between the different orbitals using Harrison's parametrization.<sup>21</sup> These changes can be interpreted as due to the stress introduced at the junction by the deformation process. One can describe this approach as a crude one-degree-of-freedom deformation of the interface that is introduced around the neck of the contact.

#### IV. DISCUSSION

Our calculated conductances for the three different geometries of Fig. 3 are given in Table I as function of distance  $d$ . In the same table, we also show the conductances calculated by neglecting the tunneling currents through the  $d$  orbitals. Our results yield an ordering of the three metals with respect to their conductances, in agreement with the sequence obtained for the experimental peaks. So, Au always has the smallest conductance, while Ni and Pt are clearly above it. If we fix the tip-sample geometry, Pt has a higher conductance than Ni for the three considered configurations. The smaller conductance in Au is a particular case illustrating the difference between noble and transition metals. The former one has no  $d$  orbitals at the Fermi level, and therefore conduction takes place mainly through  $s$  orbitals. On the other hand, transition metals have some  $d$  channels available, because those orbitals cross the Fermi level, increasing the conductance. For an  $s$  model of the tip it has been proved<sup>17</sup> that the maximum contact conductance is  $G_0$ . We argue that noble metals present a first conductance step of around  $G_0$  for those reasons, while transition metals have, as a rule, more than one quantum for the first jump: in our calculations, the maximum conductance for Pt and Ni appears for the geometry of Fig. 3(a) with an  $\sim 8\%$  reduction of the ideal distance  $d$ , and its value is close to  $3G_0$  (other experiments<sup>1,2</sup> with Al and Na also show a first jump smaller than  $G_0$ , which corroborates our prediction). This is also illustrated by the conductances shown in Table I, when the tunneling currents through the  $d$  orbitals are taken to be zero. In all the cases considered,  $G$  is smaller than  $G_0$  when the  $d$  orbitals do not contribute.

It is also interesting to mention that at long distances the tunneling current is controlled only by the  $s/p$  orbitals. This has been shown to be the case in an independent paper,<sup>22</sup> where the tunneling region between a Ni tip and a Ni surface has been analyzed. Notice that in the tunneling region, the hopping parameters decrease exponentially with distance, at variance with Harrison's law, which applies to distances close to  $d_0$ .

Regarding the different structures that can appear at the junction and their different contributions to the conductance, we obtain theoretically a large dispersion for Ni and Pt, and clearly a smaller one for Au. This also agrees with the experimental evidence found for Ni and Pt, cases showing a larger dispersion than Au.

Considering the geometries of Fig. 3 we argue based on simple mechanical stability arguments that, while the structures drawn in Figs. 3(a) and 3(b) are likely to appear in both the JC and JT processes, the structure 3(c) is more likely to appear in the pulling process. This suggests that

TABLE I. Conductance in units of  $2e^2/h$  for the geometries (a), (b), and (c) of Fig. 3.  $d/s$  refers to a calculation where the  $s$ ,  $p$ , and  $d$  orbitals are included; in the  $s$  case only the conductance through the  $s$  and  $p$  electrons has been calculated.

	Distance	(a)		(b)		(c)	
		$d/s$	$s$	$d/s$	$s$	$d/s$	$s$
Au	$0.90d_0$	1.01	0.60	0.33	0.41	0.51	0.54
	$0.95d_0$	0.88	0.597	0.37	0.46	0.61	0.62
	$1.00d_0$	0.78	0.59	0.41	0.50	0.71	0.70
	$1.05d_0$	0.71	0.57	0.44	0.53	0.79	0.76
	$1.10d_0$	0.65	0.55	0.46	0.54	0.85	0.81
Ni	$0.90d_0$	2.54	0.55	1.84	0.39	1.34	0.014
	$0.95d_0$	3.30	0.75	2.07	0.50	1.68	0.022
	$1.00d_0$	2.69	0.85	2.09	0.53	1.14	0.034
	$1.05d_0$	1.74	0.77	1.45	0.48	0.58	0.040
	$1.10d_0$	1.17	0.60	0.93	0.38	0.32	0.032
Pt	$0.90d_0$	2.08	0.65	1.32	0.81	1.37	0.11
	$0.95d_0$	3.04	0.76	1.93	0.86	1.59	0.14
	$1.00d_0$	3.16	0.85	2.45	0.87	1.40	0.18
	$1.05d_0$	2.60	0.89	2.48	0.83	0.96	0.24
	$1.10d_0$	2.02	0.88	2.15	0.76	0.68	0.30

during the JT process, geometries yielding a smaller conductance can be formed. Some support for this suggestion is also provided by our experimental data (Fig. 2), since for the JT process the conductance shows systematically a smaller value than for the JC jump.

## V. CONCLUSIONS

The experimental data presented in this paper show the important differences that appear between the conductances of the single-atom junctions formed by Au, Ni, and Pt at 4.2 K. Our theoretical analysis, based on a linear combination of atomic orbitals approach, shows that these differences can be explained by the electronic properties of the atoms forming the junction. Thus, we find that the first conductance step can be interpreted as an effect due to the electronic nature of the atom forming the neck. In particular we have shown that the relatively large conductance, appearing for transition metals such as Ni and Pt, is mainly due to the different channels afforded by the  $d$  orbitals. Because of this multichannel process, the total conductance of the single-atom junction formed by transition metals might reach values higher than

$G_0$  ranging between  $G_0$  and  $3G_0$ . For the Au junction,  $d$  bands are located deeply below the Fermi level and the conduction process occurs practically only through  $s$  orbitals (contribution of the  $p$  orbitals, located above the Fermi level, gives only about 10–20 % of the total conductance, depending on the geometry of the contact). This quasi-single-channel conductance leads to a considerably lower value of the total conductance, which should be not larger (within 10–20 % of accuracy) than  $G_0$ . In our investigation we have obtained good agreement between the experimental and theoretical results. The set of the numerical results, obtained for Au, Ni, and Pt, is ordered like the data given by the STM measurements, and also the values of the conductance, calculated for the particular metals, are in good correspondence with the experimental data.

## ACKNOWLEDGMENTS

Support by the Spanish CICYT (MAT95-1542 and PB92-0168), and the EC (CHRX-C793-0134) is acknowledged. L.J. acknowledges financial support from the Spanish Ministry of Education and Science.

\*On leave of absence from Institute of Experimental Physics, University of Wrocław, Cybulskiego 36, P-50-205 Poland.

<sup>1</sup>J.M. Krans, C.J. Muller, I.K. Yanson, Th.C.M. Govaert, R. Hesper, and J.M. van Ruitenbeek, Phys. Rev. B **48**, 14 721 (1993).

<sup>2</sup>J.M. Krans, J.M. van Ruitenbeek, V.V. Fisun, I.K. Yanson, and L.J. de Jongh, Nature **375**, 767 (1995).

<sup>3</sup>N. Agrait, J.G. Rodrigo, and S. Vieira, Phys. Rev. B **47**, 12 345 (1993).

<sup>4</sup>J.I. Pascual, J. Méndez, J. Gómez-Herrero, A.M. Baró, and N. García, Phys. Rev. Lett. **71**, 1852 (1993).

<sup>5</sup>L. Olesen, E. Laegsgaard, I. Stensgaard, F. Besenbacher, J.

Schiøtz, P. Stoltze, K.W. Jacobsen, and J.K. Nørskov, Phys. Rev. Lett. **72**, 2251 (1994).

<sup>6</sup>V.V. Dremov, S.Yu. Shapoval, and E.V. Sukhorukov, Phys. Low-Dim. Struct. **11/12**, 29 (1994).

<sup>7</sup>T.N. Todorov and A.P. Sutton, Phys. Rev. Lett. **70**, 2139 (1993).

<sup>8</sup>J.A. Torres, J.I. Pascual, and J.J. Sáenz, Phys. Rev. B **49**, 16 581 (1994).

<sup>9</sup>B.J. van Wees, H. van Houten, C.W.J. Beenakker, J.G. Williamson, L.P. Kouwenhoven, D. van der Marel, C.T. Foxon, Phys. Rev. Lett. **60**, 848 (1988).

<sup>10</sup>C. Julian Chen, Phys. Rev. Lett. **69**, 1656 (1992).

- <sup>11</sup>In our experiments it is observed that good quality tips, showing reproducible and clear topographical images, can be obtained by the procedure of formation and breakage of a crystalline connective neck between tip and sample. N. Agrait, J.G. Rodrigo, C. Sirvent, and S. Vieira, *Phys. Rev. B* **48**, 8499 (1993); N. Agrait, G. Rubio, and S. Vieira, *Phys. Rev. Lett.* **74**, 3995 (1995).
- <sup>12</sup>J.K. Gimzewski and R. Möller, *Phys. Rev. B* **36**, 1284 (1987); U. Dürig, J.K. Gimzewski, and D.W. Pohl, *Phys. Rev. Lett.* **57**, 2403 (1986); U. Dürig, O. Züger, and D.W. Pohl, *ibid.* **65**, 349 (1990).
- <sup>13</sup>C. Sirvent, J.G. Rodrigo, N. Agrait, and S. Vieira, *Physica B* **218**, 238 (1996).
- <sup>14</sup>P.L. Pernas and F. Flores, *Physica B* **175**, 221 (1991).
- <sup>15</sup>L. Martin-Moreno and J.A. Vergés, *Phys. Rev. B* **42**, 7193 (1990)
- <sup>16</sup>F. Flores, P.L. de Andrés, F.J. García Vidal, L. Jurczyszyn, N. Mingo, and R. Pérez, *Prog. Surf. Sci.* **48**, 27 (1995).
- <sup>17</sup>A. Martín-Rodero, J. Ferrer, and F. Flores, *J. Microsc.* **152**, 317 (1988).
- <sup>18</sup>L.V. Keldysh, *Zh. Éksp. Teor. Phys.* **47**, 1515 (1964) [*Sov. Phys. JETP* **20**, 1018 (1965)].
- <sup>19</sup>C. Caroli, R. Combescot, P. Nozieres, and D. Saint-James, *J. Phys. C* **4**, 916 (1971).
- <sup>20</sup>D.A. Papaconstantopoulos, *Handbook of the Band Structure of the Elemental Solids* (Plenum, New York, 1986).
- <sup>21</sup>W.A. Harrison, *Electronic Structure and Properties of Solids* (Freeman, San Francisco, 1980).
- <sup>22</sup>N. Mingo, L. Jurczyszyn, F.J. García Vidal, R. Saiz-Pardo, P.L. de Andrés, F. Flores, S.Y. Wu, and W. More, *Phys. Rev. B* (to be published).